Quantization-Loss Analysis for Array Signal-Source Localization

Manuel Stein, Amine Mezghani, Josef A. Nossek

Institute for Circuit Theory and Signal Processing,
Technische Universität München, Germany
Email: {Stein, Mezghani, Nossek}@nws.ei.tum.de

***Abstract*—This work investigates the problem of low SNR signal-source localization with an array of sensors. Keeping the receive system simple, we focus on analog-to-digital converters (ADC) with coarse resolution. In order to increase the localization accuracy and minimize the size of the receiver, we discuss the effect of analog filtering and antenna spacing on the Fisher information measure. In particular, the beneficial influence of temporal and spatial noise correlation produced by the analog receive filter and antenna coupling is considered. Results for the extreme case of 1-bit hard-limiting quantizers show that it is possible to compensate the quantization-loss of the optimum unbiased estimator through the correct choice of the analog front-end and antenna design. Further, our investigation shows that for array receivers high resolution parameter estimation is still possible with antenna spacings far below $\lambda/2$.**

***Index Terms*—1-bit hard-limiter, signal parameter estimation, antenna mutual coupling, analog filtering**

I. Introduction

In the field of signal parameter estimation, it is usually assumed that the receiver has access to digital signals with infinite resolution. While this assumption simplifies theoretic performance analysis, it implies the existence of high-resolution analog-to-digital converters (ADC). Such devices are expensive and power consuming in practice, especially when high-speed processing is required. From a circuit design perspective, hard-limiting 1-bit ADC allows to simplify the analog receiver front-end significantly. Further, the resulting binary output data makes it possible to implement digital signal processing algorithms in a very efficient way. These advantages make 1-bit ADC attractive for future signal processing devices. However, benefits come with a performance loss when comparing to receivers with higher ADC resolution. On the other hand the trend toward increasing the number of antennas makes it desirable to reduce the antenna spacing below half of the wave-length. This leads to antenna mutual coupling and spatial noise correlation. It is generally believed that both effects, coarse quantization together with antenna coupling significantly degrades the system performance. However a general analysis combining these two aspects is, to the best of our knowledge, missing in literature.

II. Related Work

The scientific discussion on signal parameter estimation from quantized data starts with the early work [1]. For low SNR signal processing applications it has been realized that the system performance with a single sensor degrades moderately by -1.96 dB [2] [3] while [4] verified that this is also true when transmitting data over a white Gaussian multiple-input multiple-output (MIMO) channel. [5] showed that the quantization-loss can be reduced for AWGN channels by oversampling the analog receive signal. Interestingly, by investigating the output-SNR of a signal correlator behind a 1-bit quantizer, [6] found that also adjusting the filter bandwidth might lead to higher system performance. [7] strengthened this inside by developing a systematic approach which allows to optimize filter bandwidth, filter shape and sampling frequency based on a Fisher information framework and attain a direct performance gain when using the optimum estimator. Recently, [8] has shown that the capacity bound of low SNR 1-bit MIMO channels with spatial noise correlation can be higher than for the case of white noise. In the context of multiple antennas [9], studied the influence of antenna coupling by setting up a circuit based model of MIMO communication systems and showed that channel capacity and antenna gain can even be higher when the antenna spacing is below $\lambda/2$. A geometric interpretation for the potential of compact antenna arrays in terms of angle-of-arrival estimation was given in [10].

III. Contribution

We provide a general Fisher information based analysis on quantized and unquantized multiple antenna systems. An important aspect of our approach is that we take into account the temporal noise correlation due to analog filtering as well as the spatial noise correlation due to antenna coupling. Following our previous work [7] [8], we derive the Fisher information measure for the estimation performance under this conditions. For a generic multi-sensor signal parameter estimation problem, with applications to radar and satellite-based navigation, we exploit the possibility of changing the noise correlation through the filter bandwidth and the antenna spacing and visualize possible performance improvements through an appropriate choice of the analog front-end and antenna design. Note, that adjusting analog parts of the receiver is in general highly attractive as this requires no additional computational effort during system operation.

IV. Problem Description

Consider a receiver equipped with an array of M sensors and a signal-source emitting a signal of known structure on a fixed carrier-frequency f_c. Receiver and source are assumed to be synchronized. The receiver would like to determine the position of the source in two dimensional space, i.e., the source's (x, y)-coordinate. To do so, the receiver measures the time-delay τ between signal transmission and reception and estimates the signal's direction-of-arrival (DOA) ζ. Combining these calculations and the knowledge on the velocity of the signal through the propagation medium, the receiver finally determines the position of the signal-source. While high precision is desirable for applications in radar or satellite-based navigation, system complexity and power consumption should be kept minimum. Therefore, this investigation assumes an extreme case: In order to save energy, signal power at the transmitter is low while the ADCs at the receiver are chosen to be the most simplest devices, i.e., symmetric 1-bit hard-limiting quantizers. Additionally the use of antenna arrays with reduced antenna spacing is attractive, especially for arrays with a large number of antennas or for small portable devices.

A. Signal Model

For the analysis an analog receive signal at M sensors

$$\boldsymbol{y}(t) = \boldsymbol{s}(t;\boldsymbol{\theta}) + \boldsymbol{n}(t) = e^{j\phi}\boldsymbol{a}(\zeta)c(t-\tau) + \boldsymbol{n}(t), \tag{1}$$

in baseband representation is assumed with parameter vector

$$\boldsymbol{\theta} = \begin{bmatrix}\phi & \zeta & \tau\end{bmatrix}^T, \tag{2}$$

and steering vector $\boldsymbol{a}(\zeta) \in \mathbb{C}^M$. $c(t-\tau) \in \mathbb{C}$ is a periodic signal of known structure which arrives at the receiver with a time-delay $\tau \in \mathbb{R}$. $\boldsymbol{n}(t) \in \mathbb{C}^M$ denotes additive noise arising at the M sensors. Filtering the analog receive signal $\boldsymbol{y}(t)$ with ideal low-pass filters of one-sided bandwidth B and sampling N times at each sensor with a sampling rate of $1/T_s \geq 2B$ with infinite ADC resolution, the stacked observation vector

$$\boldsymbol{y} = \boldsymbol{s}(\boldsymbol{\theta}) + \boldsymbol{n} = e^{j\phi}\boldsymbol{c}(\tau) \otimes \boldsymbol{a}(\zeta) + \boldsymbol{n} \in \mathbb{C}^{MN}, \tag{3}$$

is obtained where the symbol $\otimes$ denotes the Kronecker product. It is assumed that the covariance matrix of the circular symmetric noise follows the structure

$$\boldsymbol{R} = \mathrm{E}\left[\boldsymbol{n}\boldsymbol{n}^H\right] = \boldsymbol{R}_T \otimes \boldsymbol{R}_S, \tag{4}$$

which allows to divide the matrix $\boldsymbol{R}$ into a temporal part $\boldsymbol{R}_T$ and a spatial part $\boldsymbol{R}_S$. For simplicity, we assume a real-valued covariance matrix $\boldsymbol{R} = \boldsymbol{R}^*$. During the analysis $c(t)$ is chosen to be a GPS C/A (satellite 1) signal and $\frac{1}{T_s} = 2.046$ MHz.

B. Quantization Model

After sampling a symmetric hard-limiting 1-bit quantizer

$$\boldsymbol{q} = Q(\boldsymbol{y}), \tag{5}$$

performs an element-wise operation on the observation $\boldsymbol{y}$ defined by

$$Q(x) = \begin{cases} +1+\mathrm{j} & \text{if } \operatorname{Re}\{x\} \geq 0, \operatorname{Im}\{x\} \geq 0 \\ -1+\mathrm{j} & \text{if } \operatorname{Re}\{x\} < 0, \operatorname{Im}\{x\} \geq 0 \\ -1-\mathrm{j} & \text{if } \operatorname{Re}\{x\} < 0, \operatorname{Im}\{x\} < 0 \\ +1-\mathrm{j} & \text{if } \operatorname{Re}\{x\} \geq 0, \operatorname{Im}\{x\} < 0. \end{cases} \tag{6}$$

Paper [8] showed that with the orthogonality principle [11, p.177] and a low SNR assumption, the output $\boldsymbol{q}$ can be approximated

$$\boldsymbol{q} = \boldsymbol{Q}\boldsymbol{y} + \boldsymbol{e} = \boldsymbol{Q}\boldsymbol{s}(\boldsymbol{\theta}) + \boldsymbol{Q}\boldsymbol{n} + \boldsymbol{e} = \boldsymbol{s}_q(\boldsymbol{\theta}) + \boldsymbol{n}_q, \tag{7}$$

with the effective noise correlation matrix

$$\begin{aligned}\boldsymbol{R}_q &= \mathrm{E}\left[\boldsymbol{n}_q\boldsymbol{n}_q^H\right] \\ &= \frac{2}{\pi}\arcsin\left(\operatorname{diag}\left(\boldsymbol{R}^{-\frac{1}{2}}\right)\boldsymbol{R}\operatorname{diag}\left(\boldsymbol{R}^{-\frac{1}{2}}\right)\right),\end{aligned} \tag{8}$$

and the effective gain

$$\boldsymbol{Q} = \sqrt{\frac{2}{\pi}}\operatorname{diag}\left(\boldsymbol{R}\right)^{-\frac{1}{2}}. \tag{9}$$

C. Pessimistic Equivalent System

Note that (8) only specifies the second moment of the underlying density function of the effective additive noise behind the quantization device. Nevertheless, it can be shown that the worst-case estimation theoretical characterization [12] of the parameterized probability density function (pdf) associated with the digital receive signal $\boldsymbol{q}$ is given by a colored Gaussian distribution

$$p(\boldsymbol{q};\boldsymbol{\theta}) = \frac{1}{\pi^N \det \boldsymbol{R}_q}\exp\left[-(\boldsymbol{q}-\boldsymbol{s}_q(\boldsymbol{\theta}))^H\boldsymbol{R}_q^{-1}(\boldsymbol{q}-\boldsymbol{s}_q(\boldsymbol{\theta}))\right],$$

with zero mean. Consequently, in order to guarantee robustness of our results this pessimistic assumption is used.

V. Noise Correlation

A. Temporal Noise Correlation

Assuming white Gaussian noise with constant power spectral density N_0, the temporal auto-correlation function of the additive noise at the m-th sensor after low-pass filtering

$$r_m(t) = \int_{-\infty}^{\infty}\boldsymbol{n}_m(t)\boldsymbol{n}_m^\star(\nu - t)\mathrm{d}\nu, \tag{10}$$

can be characterized by the inverse Fourier transform of the auto-correlation function in the frequency domain

$$\begin{aligned} r_m(t) &= \frac{1}{2\pi}\int_{-\infty}^{\infty}N_0\left|H(\omega)\right|^2 e^{-\mathrm{j}\omega\mathrm{t}}\mathrm{d}\omega \\ &= 2BN_0\operatorname{sinc}\left(2Bt\right),\end{aligned} \tag{11}$$

where

$$\operatorname{sinc}(x) = \frac{\sin(\pi x)}{\pi x}, \tag{12}$$

and the transfer function of the ideal low-pass filter is

$$H(\omega) = \begin{cases} 1 & \text{if } |\omega| \leq 2\pi B \\ 0 & \text{else.} \end{cases} \quad (13)$$

Consequently, the temporal covariance matrix $\boldsymbol{R}_T$ of the noise at each of the M sensors is given by

$$[\boldsymbol{R}_T]_{ik} = 2BN_0 \operatorname{sinc}\left(2BT_s\,|i-k|\right). \quad (14)$$

It is observed that temporally white noise, i.e.,

$$\boldsymbol{R}_T = 2BN_0 \boldsymbol{I}_N, \quad (15)$$

is only obtained if the equality $T_s = \frac{1}{2B}$ is satisfied exactly.

B. Spatial Noise Correlation

In interference free scenarios, it is usually assumed that the noise is spatially white

$$\boldsymbol{R}_S = \boldsymbol{I}_M, \quad (16)$$

while the array sensors are placed at a distance of $d = \frac{1}{2}$, normalize with respect to the wave-length λ. Assuming a uniform linear array (ULA) with isotropic dipoles and dominant isotropic background radiation noise (in comparison to the noise of the amplifiers), we obtain the following physically consistent spatial correlation model [9]

$$\boldsymbol{R}_S = \boldsymbol{C}_M, \quad (17)$$

with

$$\boldsymbol{C}_M = \begin{bmatrix} 1 & \operatorname{sinc}(2d) & \operatorname{sinc}(4d) & \dots \\ \operatorname{sinc}(2d) & 1 & \operatorname{sinc}(2d) & \ddots \\ \operatorname{sinc}(4d) & \operatorname{sinc}(2d) & 1 & \ddots \\ \ddots & \ddots & \ddots & \ddots \end{bmatrix} \in \mathbb{R}^{M \times M}, \quad (18)$$

which characterizes noise correlation in relation to the distance d between the antenna elements.

VI. Estimation Performance

Given the parameterized pdf $p(\boldsymbol{q};\boldsymbol{\theta})$ and assuming deterministic but unknown parameters $\boldsymbol{\theta}$, the optimum unbiased estimator $\hat{\boldsymbol{\theta}}(\boldsymbol{q})$ is the maximum-likelihood estimator (MLE)

$$\hat{\boldsymbol{\theta}}(\boldsymbol{q}) = \arg\max_{\boldsymbol{\theta}} p(\boldsymbol{q};\boldsymbol{\theta}), \quad (19)$$

while the conditional mean square error (MSE) matrix

$$\boldsymbol{R}_{\epsilon\epsilon}(\boldsymbol{\theta}) = \mathrm{E}_{\boldsymbol{q}|\boldsymbol{\theta}}\left[(\hat{\boldsymbol{\theta}}(\boldsymbol{q}) - \boldsymbol{\theta})(\hat{\boldsymbol{\theta}}(\boldsymbol{q}) - \boldsymbol{\theta})^T\right], \quad (20)$$

characterizes the estimation errors of the MLE and their mutual correlation.

A. Performance Bound

As a direct characterization of $\boldsymbol{R}_{\epsilon\epsilon}(\boldsymbol{\theta})$ is in general difficult, the error analysis is here based on theoretical performance bounds of the individual estimation errors. The entries of $\boldsymbol{R}_{\epsilon\epsilon}(\boldsymbol{\theta})$ can be bounded through the Cramer-Rao lower bound (CRLB) [13]

$$[\boldsymbol{R}_{\epsilon\epsilon}(\boldsymbol{\theta})]_{ik} \geq [\boldsymbol{F}_q^{-1}(\boldsymbol{\theta})]_{ik}, \quad (21)$$

which is attained by inverting the Fisher information matrix

$$\begin{aligned} [\boldsymbol{F}_q(\boldsymbol{\theta})]_{ik} &= 2 \cdot \mathrm{Re}\left\{ \frac{\partial \boldsymbol{s}_q^H(\boldsymbol{\theta})}{\partial \boldsymbol{\theta}_i} \boldsymbol{R}_q^{-1} \frac{\partial \boldsymbol{s}_q(\boldsymbol{\theta})}{\partial \boldsymbol{\theta}_k} \right\} && (22) \\ &= 2 \cdot \mathrm{Re}\left\{ \frac{\partial \boldsymbol{s}^H(\boldsymbol{\theta})}{\partial \boldsymbol{\theta}_i} \boldsymbol{Q}^H \boldsymbol{R}_q^{-1} \boldsymbol{Q} \frac{\partial \boldsymbol{s}(\boldsymbol{\theta})}{\partial \boldsymbol{\theta}_k} \right\} && (23) \\ &= 2 \cdot \mathrm{Re}\left\{ \frac{\partial \boldsymbol{s}^H(\boldsymbol{\theta})}{\partial \boldsymbol{\theta}_i} \boldsymbol{Q}^H \boldsymbol{R}_q^{-1} \boldsymbol{Q} \frac{\partial \boldsymbol{s}(\boldsymbol{\theta})}{\partial \boldsymbol{\theta}_k} \right\}. && (24) \end{aligned}$$

In the low SNR regime, the CRLB matches the real estimation performance of the MLE if the observation length N is chosen sufficiently large. For the considered system model the following holds

$$\begin{aligned} [\boldsymbol{F}_q(\boldsymbol{\theta})]_{11} &= 2 \cdot \mathrm{Re}\left\{ \frac{\partial \boldsymbol{s}^H(\boldsymbol{\theta})}{\partial \phi} \boldsymbol{Q}^H \boldsymbol{R}_q^{-1} \boldsymbol{Q} \frac{\partial \boldsymbol{s}(\boldsymbol{\theta})}{\partial \phi} \right\} \\ [\boldsymbol{F}_q(\boldsymbol{\theta})]_{12/21} &= 2 \cdot \mathrm{Re}\left\{ \frac{\partial \boldsymbol{s}^H(\boldsymbol{\theta})}{\partial \phi} \boldsymbol{Q}^H \boldsymbol{R}_q^{-1} \boldsymbol{Q} \frac{\partial \boldsymbol{s}(\boldsymbol{\theta})}{\partial \zeta} \right\} \\ [\boldsymbol{F}_q(\boldsymbol{\theta})]_{13/31} &= 2 \cdot \mathrm{Re}\left\{ \frac{\partial \boldsymbol{s}^H(\boldsymbol{\theta})}{\partial \phi} \boldsymbol{Q}^H \boldsymbol{R}_q^{-1} \boldsymbol{Q} \frac{\partial \boldsymbol{s}(\boldsymbol{\theta})}{\partial \tau} \right\} \\ [\boldsymbol{F}_q(\boldsymbol{\theta})]_{22} &= 2 \cdot \mathrm{Re}\left\{ \frac{\partial \boldsymbol{s}^H(\boldsymbol{\theta})}{\partial \zeta} \boldsymbol{Q}^H \boldsymbol{R}_q^{-1} \boldsymbol{Q} \frac{\partial \boldsymbol{s}(\boldsymbol{\theta})}{\partial \zeta} \right\} \\ [\boldsymbol{F}_q(\boldsymbol{\theta})]_{23/32} &= 2 \cdot \mathrm{Re}\left\{ \frac{\partial \boldsymbol{s}^H(\boldsymbol{\theta})}{\partial \zeta} \boldsymbol{Q}^H \boldsymbol{R}_q^{-1} \boldsymbol{Q} \frac{\partial \boldsymbol{s}(\boldsymbol{\theta})}{\partial \tau} \right\} \\ [\boldsymbol{F}_q(\boldsymbol{\theta})]_{33} &= 2 \cdot \mathrm{Re}\left\{ \frac{\partial \boldsymbol{s}^H(\boldsymbol{\theta})}{\partial \tau} \boldsymbol{Q}^H \boldsymbol{R}_q^{-1} \boldsymbol{Q} \frac{\partial \boldsymbol{s}(\boldsymbol{\theta})}{\partial \tau} \right\}, && (25) \end{aligned}$$

where

$$\begin{aligned} \frac{\partial \boldsymbol{s}(\boldsymbol{\theta})}{\partial \phi} &= j e^{j\phi}\Big(\boldsymbol{c}(\tau) \otimes \boldsymbol{a}(\zeta)\Big) \\ \frac{\partial \boldsymbol{s}(\boldsymbol{\theta})}{\partial \zeta} &= e^{j\phi}\Big(\boldsymbol{c}(\tau) \otimes \frac{\partial \boldsymbol{a}(\zeta)}{\partial \zeta}\Big) \\ \frac{\partial \boldsymbol{s}(\boldsymbol{\theta})}{\partial \tau} &= e^{j\phi}\Big(\frac{\partial \boldsymbol{c}(\tau)}{\partial \tau} \otimes \boldsymbol{a}(\zeta)\Big). && (26) \end{aligned}$$

With a large number of samples [7]

$$\begin{aligned} \boldsymbol{c}^H(\tau)\boldsymbol{R}\boldsymbol{c}(\tau) &= \text{const.} \\ \frac{\partial \boldsymbol{c}^H(\tau)}{\partial \tau}\boldsymbol{R}\frac{\partial \boldsymbol{c}(\tau)}{\partial \tau} &= \text{const.} \\ \frac{\partial \boldsymbol{c}^H(\tau)}{\partial \tau}\boldsymbol{R}\boldsymbol{c}(\tau) = \boldsymbol{c}^H(\tau)\boldsymbol{R}\frac{\partial \boldsymbol{c}(\tau)}{\partial \tau} &= 0, && (27) \end{aligned}$$

for an arbitrary covariance matrix $\boldsymbol{R}$ such that in the following, we use the simplistic notation

$$\begin{aligned} \boldsymbol{c}(\tau) &= \boldsymbol{c} \\ \frac{\partial \boldsymbol{c}^H(\tau)}{\partial \tau} &= \partial \boldsymbol{c}. && (28) \end{aligned}$$

VII. Performance Analysis - Two Antennas

For a first performance discussion, we choose a two antenna ULA receiver with a steering vector

$$\boldsymbol{a}(\zeta) = \begin{bmatrix} 1 & e^{-\mathrm{j}2\pi \mathrm{d} \cos(\zeta)} \end{bmatrix}^T, \tag{29}$$

thus

$$\frac{\partial \boldsymbol{a}(\zeta)}{\partial \zeta} = \begin{bmatrix} 0 & \mathrm{j}2\pi \mathrm{d} \sin(\zeta) \mathrm{e}^{-\mathrm{j}2\pi \mathrm{d} \cos(\zeta)} \end{bmatrix}^T, \tag{30}$$

while the identities

$$\begin{aligned} \boldsymbol{a}^H(\zeta)\boldsymbol{a}(\zeta) &= 2 \\ \frac{\partial \boldsymbol{a}^H(\zeta)}{\partial \zeta}\frac{\partial \boldsymbol{a}(\zeta)}{\partial \zeta} &= (2\pi d)^2 \sin^2(\zeta) \\ \boldsymbol{a}^H(\zeta)\frac{\partial \boldsymbol{a}(\zeta)}{\partial \zeta} &= \mathrm{j}2\pi \mathrm{d} \sin(\zeta) \\ \frac{\partial \boldsymbol{a}^H(\zeta)}{\partial \zeta}\boldsymbol{a}(\zeta) &= -\mathrm{j}2\pi \mathrm{d} \sin(\zeta), \end{aligned} \tag{31}$$

are verified easily. The time-space covariance matrix has in general the structure

$$\boldsymbol{R} = \begin{bmatrix} \boldsymbol{R}_1 & \boldsymbol{R}_2 \\ \boldsymbol{R}_2 & \boldsymbol{R}_1 \end{bmatrix}, \tag{32}$$

such that

$$\boldsymbol{R}^{-1} = \begin{bmatrix} (\boldsymbol{R}_1 - \boldsymbol{R}_2\boldsymbol{R}_1^{-1}\boldsymbol{R}_2)^{-1} & (\boldsymbol{R}_2 - \boldsymbol{R}_1\boldsymbol{R}_2^{-1}\boldsymbol{R}_1)^{-1} \\ (\boldsymbol{R}_2 - \boldsymbol{R}_1\boldsymbol{R}_2^{-1}\boldsymbol{R}_1)^{-1} & (\boldsymbol{R}_1 - \boldsymbol{R}_2\boldsymbol{R}_1^{-1}\boldsymbol{R}_2)^{-1} \end{bmatrix}. \tag{33}$$

In the following we define for brevity

$$\boldsymbol{R}' = \begin{bmatrix} \boldsymbol{R}_1' & \boldsymbol{R}_2' \\ \boldsymbol{R}_2' & \boldsymbol{R}_1' \end{bmatrix} = \begin{cases} \boldsymbol{Q}^H\boldsymbol{R}_q^{-1}\boldsymbol{Q} & \text{(1-bit receiver)} \\ \boldsymbol{R}^{-1} & \text{(unquantized receiver).} \end{cases} \tag{34}$$

For the entries of $\boldsymbol{F}(\boldsymbol{\theta})$, we calculate

$$\begin{aligned} &\left(\mathrm{j}\mathrm{e}^{\mathrm{j}\phi}\boldsymbol{c} \otimes \boldsymbol{a}(\zeta)\right)^{\mathrm{H}} \boldsymbol{R}' \left(\mathrm{j}\mathrm{e}^{\mathrm{j}\phi}\boldsymbol{c} \otimes \boldsymbol{a}(\zeta)\right) = \\ &\qquad 2 \cdot \boldsymbol{c}^H\left(\boldsymbol{R}_1' + \cos\left(2\pi d \cos(\zeta)\right)\boldsymbol{R}_2'\right)\boldsymbol{c}, \end{aligned}$$

such that

$$[\boldsymbol{F}(\boldsymbol{\theta})]_{11} = 4 \cdot \boldsymbol{c}^H\left(\boldsymbol{R}_1' + \cos\left(2\pi d \cos(\zeta)\right)\boldsymbol{R}_2'\right)\boldsymbol{c}, \tag{35}$$

and

$$\begin{aligned} &\left(\mathrm{j}\mathrm{e}^{\mathrm{j}\phi}\boldsymbol{c} \otimes \boldsymbol{a}(\zeta)\right)^{\mathrm{H}} \boldsymbol{R}' \left(e^{j\phi}\boldsymbol{c} \otimes \frac{\partial \boldsymbol{a}(\zeta)}{\partial \zeta}\right) = \\ &\qquad 2\pi d \sin(\zeta) \cdot \boldsymbol{c}^H\left(\boldsymbol{R}_1' + e^{-\mathrm{j}2\pi \mathrm{d} \cos(\zeta)}\boldsymbol{R}_2'\right)\boldsymbol{c}, \end{aligned}$$

such that

$$\begin{aligned} [\boldsymbol{F}(\boldsymbol{\theta})]_{12} &= 4\pi d \sin(\zeta) \cdot \boldsymbol{c}^H\left(\boldsymbol{R}_1' + \mathrm{Re}\left\{e^{-\mathrm{j}2\pi \mathrm{d} \cos(\zeta)}\right\}\boldsymbol{R}_2'\right)\boldsymbol{c} \\ &= 4\pi d \sin(\zeta) \cdot \boldsymbol{c}^H\left(\boldsymbol{R}_1' + \cos(2\pi d \cos(\zeta))\boldsymbol{R}_2'\right)\boldsymbol{c} \\ &= [\boldsymbol{F}(\boldsymbol{\theta})]_{21}, \end{aligned} \tag{36}$$

and

$$\left(\mathrm{j}\mathrm{e}^{\mathrm{j}\phi}\boldsymbol{c} \otimes \boldsymbol{a}(\zeta)\right)^{\mathrm{H}} \boldsymbol{R}' \left(\mathrm{e}^{\mathrm{j}\phi}\partial\boldsymbol{c}^{\mathrm{H}} \otimes \boldsymbol{a}(\zeta)\right) = 0,$$

giving

$$[\boldsymbol{F}(\boldsymbol{\theta})]_{13} = [\boldsymbol{F}(\boldsymbol{\theta})]_{31} = 0, \tag{37}$$

and

$$\left(e^{j\phi}\boldsymbol{c} \otimes \frac{\partial \boldsymbol{a}(\zeta)}{\partial \zeta}\right)^H \boldsymbol{R}' \left(e^{j\phi}\partial\boldsymbol{c}^H \otimes \boldsymbol{a}(\zeta)\right) = 0,$$

leading to

$$[\boldsymbol{F}(\boldsymbol{\theta})]_{23} = [\boldsymbol{F}(\boldsymbol{\theta})]_{32} = 0, \tag{38}$$

and

$$\begin{aligned} &\left(e^{j\phi}\boldsymbol{c} \otimes \frac{\partial \boldsymbol{a}(\zeta)}{\partial \zeta}\right)^H \boldsymbol{R}' \left(e^{j\phi}\boldsymbol{c} \otimes \frac{\partial \boldsymbol{a}(\zeta)}{\partial \zeta}\right) = \\ &\qquad = (2\pi d)^2 \sin^2(\zeta) \cdot \boldsymbol{c}^H\boldsymbol{R}_1'\boldsymbol{c}, \end{aligned}$$

resulting in

$$[\boldsymbol{F}(\boldsymbol{\theta})]_{22} = 2(2\pi d)^2 \sin^2(\zeta) \cdot \boldsymbol{c}^H\boldsymbol{R}_1'\boldsymbol{c}, \tag{39}$$

and finally

$$\begin{aligned} &\left(e^{j\phi}\frac{\partial \boldsymbol{c}}{\partial \tau} \otimes \boldsymbol{a}(\zeta)\right)^H \boldsymbol{R}' \left(e^{j\phi}\frac{\partial \boldsymbol{c}}{\partial \tau} \otimes \boldsymbol{a}(\zeta)\right) = \\ &\qquad = 2 \cdot \partial\boldsymbol{c}^H\left(\boldsymbol{R}_1' + \cos\left(2\pi d \cos(\zeta)\right)\boldsymbol{R}_2'\right)\partial\boldsymbol{c}, \end{aligned}$$

such that

$$[\boldsymbol{F}(\boldsymbol{\theta})]_{33} = 4 \cdot \partial\boldsymbol{c}^H\left(\boldsymbol{R}_1' + \cos\left(2\pi d \cos(\zeta)\right)\boldsymbol{R}_2'\right)\partial\boldsymbol{c}. \tag{40}$$

The CRLB for ζ and τ are given by

$$\begin{aligned} [\boldsymbol{F}(\boldsymbol{\theta})^{-1}]_{22} &= \frac{[\boldsymbol{F}(\boldsymbol{\theta})]_{11}}{[\boldsymbol{F}(\boldsymbol{\theta})]_{11}[\boldsymbol{F}(\boldsymbol{\theta})]_{22} - [\boldsymbol{F}(\boldsymbol{\theta})]_{12}^2} \\ &= \frac{1}{(2\pi d)^2 \sin^2(\zeta) \cdot \boldsymbol{c}^H\left(\boldsymbol{R}_1' - \cos(2\pi d \cos(\zeta))\boldsymbol{R}_2'\right)\boldsymbol{c}} \\ [\boldsymbol{F}(\boldsymbol{\theta})^{-1}]_{33} &= \frac{1}{[\boldsymbol{F}(\boldsymbol{\theta})]_{33}} \\ &= \frac{1}{4}\frac{1}{\partial\boldsymbol{c}^H\left(\boldsymbol{R}_1' + \cos\left(2\pi d \cos(\zeta)\right)\boldsymbol{R}_2'\right)\partial\boldsymbol{c}}. \end{aligned} \tag{41}$$

A. Ideal Receiver - Variable Antenna Spacing

Before turning our attention onto quantized receive systems, we verify the impact of the antenna spacing on the estimation performance. Therefore we fix $B = \frac{1}{2T_s}$ and vary the antenna spacing within $0 < d \leq \frac{1}{2}$. For this setting, we obtain

$$\begin{aligned} \boldsymbol{R}' &= (\boldsymbol{R}_T \otimes \boldsymbol{R}_S)^{-1} = \left(BN_0\boldsymbol{I}_N \otimes \boldsymbol{C}_M\right)^{-1} \\ &= \frac{1}{BN_0}\begin{bmatrix} \boldsymbol{I}_N & \mathrm{sinc}(2d)\,\boldsymbol{I}_N \\ \mathrm{sinc}(2d)\,\boldsymbol{I}_N & \boldsymbol{I}_N \end{bmatrix}^{-1}, \end{aligned} \tag{42}$$

such that

$$\begin{aligned} \boldsymbol{R}_1' &= \frac{1}{BN_0}\frac{1}{(1 - \mathrm{sinc}^2(2d))}\boldsymbol{I}_N \\ \boldsymbol{R}_2' &= -\frac{1}{BN_0}\frac{\mathrm{sinc}(2d)}{(1 - \mathrm{sinc}^2(2d))}\boldsymbol{I}_N, \end{aligned} \tag{43}$$

and the CRLBs can be written as

$$
\begin{aligned}
[\boldsymbol{F}_{\infty}(\boldsymbol{\theta})^{-1}]_{22} &= = \frac{BN_0}{(2\pi d)^2 \sin^2(\zeta)\, \boldsymbol{c}^H \boldsymbol{c}} f_{\infty,\zeta}(d,\zeta) \\
[\boldsymbol{F}_{\infty}(\boldsymbol{\theta})^{-1}]_{33} &= \frac{1}{4} \frac{BN_0}{\partial \boldsymbol{c}^H \partial \boldsymbol{c}} f_{\infty,\tau}(d,\zeta),
\end{aligned}
\tag{44}
$$

with

$$
\begin{aligned}
f_{\infty,\zeta}(d,\zeta) &= \frac{\left(1-\operatorname{sinc}^2(2d)\right)}{\left(1+\cos(2\pi d \cos(\zeta))\operatorname{sinc}(2d)\right)} \\
f_{\infty,\tau}(d,\zeta) &= \frac{\left(1-\operatorname{sinc}^2(2d)\right)}{\left(1-\cos(2\pi d \cos(\zeta))\operatorname{sinc}(2d)\right)}.
\end{aligned}
\tag{45}
$$

Comparing this system of infinite resolution to a system with $d = \frac{1}{2}$ the following performance measures can be defined

$$
\begin{aligned}
\chi_{\infty,\zeta}(\boldsymbol{\theta}) &= \frac{[\boldsymbol{F}_{\infty}^{-1}(\boldsymbol{\theta})]_{22}\big|_{d=\frac{1}{2}}}{[\boldsymbol{F}_{\infty}^{-1}(\boldsymbol{\theta})]_{22}} = \frac{(2d)^2}{f_{\infty,\zeta}(d,\zeta)} \\
\chi_{\infty,\tau}(\boldsymbol{\theta}) &= \frac{[\boldsymbol{F}_{\infty}^{-1}(\boldsymbol{\theta})]_{33}\big|_{d=\frac{1}{2}}}{[\boldsymbol{F}_{\infty}^{-1}(\boldsymbol{\theta})]_{33}} = \frac{1}{f_{\infty,\tau}(d,\zeta)}.
\end{aligned}
\tag{46}
$$

Fig. 1 shows the performance for the estimation of ζ as function of the antenna spacing. Interestingly, we observe only a moderate degradation in the estimation performance when the distance d goes to zero. This is in accordance with the result of [10]. Remarkably, for estimating the delay τ even an improvement (Fig. 2) in the performance for certain DOAs (especially close to the end-fire direction) can be obtained when decreasing the antenna spacing below $\lambda/2$. This is explained by the increased antenna gain (super gain) [9].

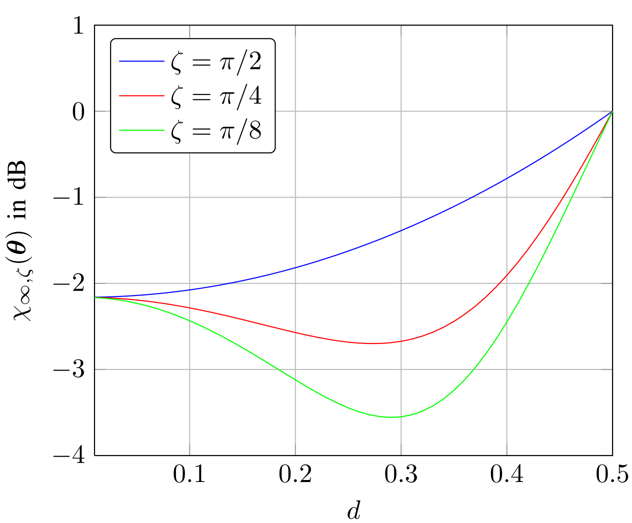

Fig. 1. Performance Ratio in ζ vs. Spacing

B. 1-bit Receiver - Variable Antenna Spacing

For a 1-bit receiver with fixed bandwidth $B = \frac{1}{2T_s}$ and an antenna spacing $0 < d \leq \frac{1}{2}$ we obtain

$$
\boldsymbol{R}' = \frac{1}{BN_0} \arcsin\left(\boldsymbol{I}_N \otimes \boldsymbol{C}_M\right)^{-1},
\tag{47}
$$

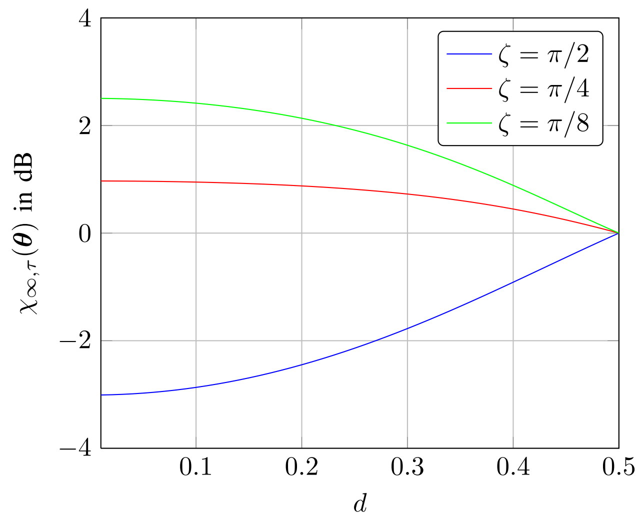

Fig. 2. Performance Ratio in τ vs. Spacing

such that

$$
\boldsymbol{R}_1' = \frac{\frac{\pi}{2}}{BN_0\left(\left(\frac{\pi}{2}\right)^2 - \arcsin^2(\operatorname{sinc}(2d))\right)} \boldsymbol{I}_N
\tag{48}
$$

$$
\boldsymbol{R}_2' = -\frac{\arcsin(\operatorname{sinc}(2d))}{BN_0\left(\left(\frac{\pi}{2}\right)^2 - \arcsin^2(\operatorname{sinc}(2d))\right)} \boldsymbol{I}_N.
\tag{49}
$$

For this setting the CRLBs are

$$
\begin{aligned}
[\boldsymbol{F}_{q}(\boldsymbol{\theta})^{-1}]_{22} &= \frac{BN_0}{(2\pi d)^2 \sin^2(\zeta)\, \boldsymbol{c}^H \boldsymbol{c}} f_{q,\zeta}(d,\zeta) \\
[\boldsymbol{F}_{q}(\boldsymbol{\theta})^{-1}]_{33} &= \frac{1}{4} \frac{BN_0}{\partial \boldsymbol{c}^H \partial \boldsymbol{c}} f_{q,\tau}(d,\zeta),
\end{aligned}
\tag{50}
$$

with

$$
\begin{aligned}
f_{q,\zeta}(d,\zeta) &= \frac{\left(\left(\frac{\pi}{2}\right)^2 - \arcsin^2(\operatorname{sinc}(2d))\right)}{\left(\frac{\pi}{2} + \cos(2\pi d \cos(\zeta))\arcsin(\operatorname{sinc}(2d))\right)} \\
f_{q,\tau}(d,\tau) &= \frac{\left(\left(\frac{\pi}{2}\right)^2 - \arcsin^2(\operatorname{sinc}(2d))\right)}{\left(\frac{\pi}{2} - \cos(2\pi d \cos(\zeta))\arcsin(\operatorname{sinc}(2d))\right)}.
\end{aligned}
\tag{51}
$$

Compared to an unquantized system with $d = \frac{1}{2}$, the relative performance can be measures by

$$
\begin{aligned}
\chi_{q,\zeta}(\boldsymbol{\theta}) &= \frac{[\boldsymbol{F}_{\infty}^{-1}(\boldsymbol{\theta})]_{22}\big|_{d=\frac{1}{2}}}{[\boldsymbol{F}_{q}^{-1}(\boldsymbol{\theta})]_{22}} = \frac{(2d)^2}{f_{q,\zeta}(d,\zeta)} \\
\chi_{q,\tau}(\boldsymbol{\theta}) &= \frac{[\boldsymbol{F}_{\infty}^{-1}(\boldsymbol{\theta})]_{33}\big|_{d=\frac{1}{2}}}{[\boldsymbol{F}_{q}^{-1}(\boldsymbol{\theta})]_{33}} = \frac{1}{f_{q,\tau}(d,\zeta)}.
\end{aligned}
\tag{52}
$$

Validating the performance at $d = \frac{1}{2}$ the well-known quantization-loss of factor $\frac{2}{\pi}$ can be verified

$$
\chi_{q,\zeta}(\boldsymbol{\theta})\big|_{d=\frac{1}{2}} = \chi_{q,\tau}(\boldsymbol{\theta})\big|_{d=\frac{1}{2}} = \frac{2}{\pi} \quad (-1.96 \text{ dB}).
\tag{53}
$$

Note that in this situation, the loss does not depend on the parameter constellation $\boldsymbol{\theta}$, in particular ζ. In Fig. 3, the performance ratio in terms of estimating ζ is depicted. Contrary to the unquantized case, the performance degradation becomes less sensitive to the specific DOA. In particular a small decrease in the antenna spacing does not effect to much the end-fire directions compared to the unquantized case. However, in terms of time-delay estimation the behavior of the estimation performance, by slightly decreasing the antenna distance, is similar to the unquantized case, justified again by the higher antenna gain. Nevertheless, a significant loss is obtained when the spacing is decrease drastically.

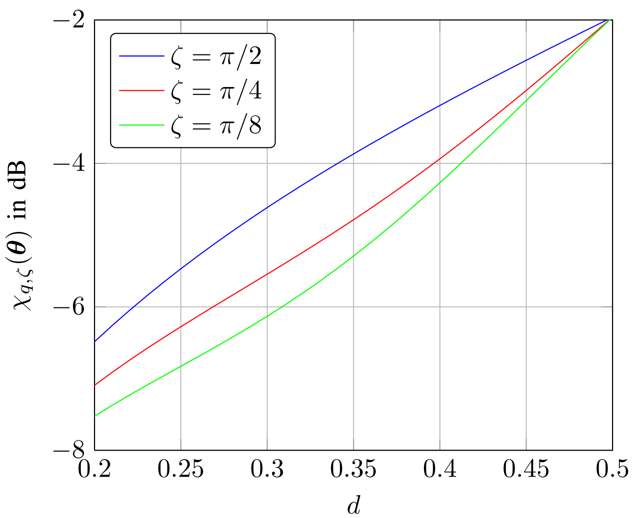

Fig. 3. 1-bit Performance Ratio in ζ vs. Spacing

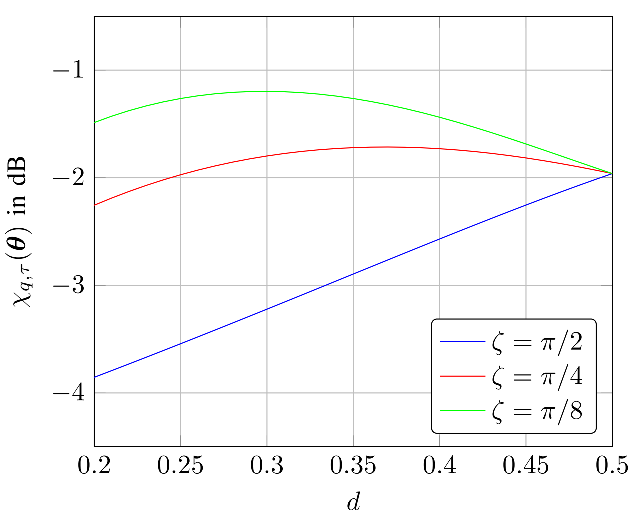

Fig. 4. 1-bit Performance Ratio in τ vs. Spacing

C. 1-bit Receiver - Variable Filter Bandwidth

Now we investigate the possibility of adapting the analog filter bandwidth $B = \frac{\rho}{2T_s}$ with $0 \leq \rho \leq 1$ [7] while the antenna spacing is fixed to $d = \frac{1}{2}$. The space-time matrix is given by

$$\boldsymbol{R}' = \frac{1}{\rho B N_0} \arcsin\left(\frac{1}{\rho B N_0}\boldsymbol{R}_T \otimes \boldsymbol{I}_M\right)^{-1}, \qquad (54)$$

such that

$$\begin{aligned} \boldsymbol{R}'_1 &= \frac{1}{\rho B N_0} \arcsin\left(\frac{1}{\rho B N_0}\boldsymbol{R}_T\right)^{-1} \\ \boldsymbol{R}'_2 &= \boldsymbol{0}_N. \end{aligned} \qquad (55)$$

Here the CRLBs attain the following form

$$\begin{aligned} [\boldsymbol{F}_q(\boldsymbol{\theta})^{-1}]_{22} &= \frac{\rho B N_0}{\pi^2 \sin^2(\zeta)\, \boldsymbol{c}_\rho^H \arcsin\left(\frac{1}{\rho B N_0}\boldsymbol{R}_T\right)^{-1} \boldsymbol{c}_\rho} \\ [\boldsymbol{F}_q(\boldsymbol{\theta})^{-1}]_{33} &= \frac{1}{4}\frac{\rho B N_0}{\partial \boldsymbol{c}_\rho^H \arcsin\left(\frac{1}{\rho B N_0}\boldsymbol{R}_T\right)^{-1} \partial \boldsymbol{c}_\rho}, \end{aligned} \qquad (56)$$

where $\boldsymbol{c}_\rho$ and $\partial\boldsymbol{c}_\rho$ are the signal and its derivative after filtering by a low-pass filter with one-sided bandwidth $B = \frac{\rho}{2T_s}$. The relative performance with respect to an ideal system with infinite resolution can be characterized by

$$\begin{aligned} \chi_{q,\zeta}(\boldsymbol{\theta}) &= \frac{1}{\rho}\frac{\boldsymbol{c}_\rho^H \arcsin\left(\frac{1}{\rho B N_0}\boldsymbol{R}_T\right)^{-1} \boldsymbol{c}_\rho}{\boldsymbol{c}^H \boldsymbol{c}} \\ \chi_{q,\tau}(\boldsymbol{\theta}) &= \frac{1}{\rho}\frac{\partial\boldsymbol{c}_\rho^H \arcsin\left(\frac{1}{\rho B N_0}\boldsymbol{R}_T\right)^{-1} \partial\boldsymbol{c}_\rho}{\partial\boldsymbol{c}^H \partial\boldsymbol{c}}. \end{aligned} \qquad (57)$$

In Fig. 5 the performance ratios in terms of the estimation of ζ and τ are shown. In accordance with [7], a reduction of the filter bandwidth B below the Nyquist rate can be beneficial.

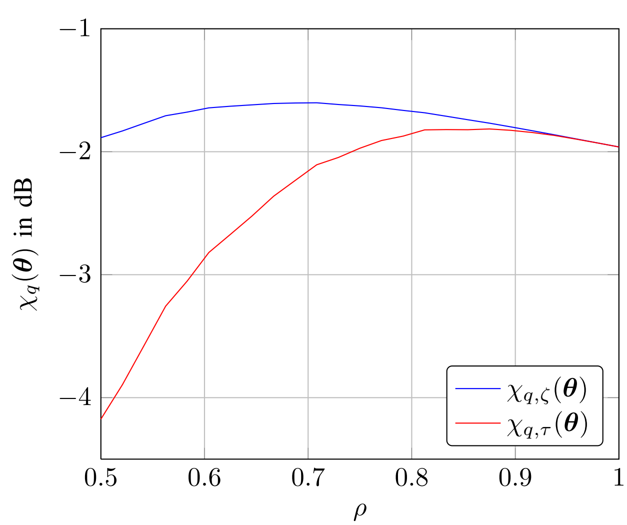

Fig. 5. 1-bit Performance Ratio in ζ and τ vs. Bandwidth

D. 1-bit Receiver - Variable Spacing and Bandwidth

Next, the case of a receiver with variable bandwidth $B = \frac{\rho}{2T_s}$, $0 \leq \rho \leq 1$ and variable antenna spacing $0 < d \leq \frac{1}{2}$ is considered. Here

$$\boldsymbol{R}' = \frac{1}{\rho B N_0} \arcsin\left(\frac{1}{\rho B N_0}\boldsymbol{R}_T \otimes \boldsymbol{C}_M\right)^{-1}, \tag{58}$$

such that

$$\begin{aligned}\boldsymbol{R}_1' &= \frac{1}{\rho B N_0}\left(\boldsymbol{R}_A' - \boldsymbol{R}_B'\boldsymbol{R}_A'^{-1}\boldsymbol{R}_B'\right)^{-1} = \frac{1}{\rho B N_0}\boldsymbol{R}_1''\\ \boldsymbol{R}_2' &= \frac{1}{\rho B N_0}\left(\boldsymbol{R}_B' - \boldsymbol{R}_A'\boldsymbol{R}_B'^{-1}\boldsymbol{R}_A'\right)^{-1} = \frac{1}{\rho B N_0}\boldsymbol{R}_2'',\end{aligned} \tag{59}$$

with

$$\begin{aligned}\boldsymbol{R}_A' &= \arcsin\left(\frac{1}{\rho B N_0}\boldsymbol{R}_T\right)\\ \boldsymbol{R}_B' &= \arcsin\left(\frac{\operatorname{sinc}(2d)}{\rho B N_0}\boldsymbol{R}_T\right),\end{aligned} \tag{60}$$

such that the CRLBs are given by

$$\begin{aligned}[\boldsymbol{F}_q(\boldsymbol{\theta})^{-1}]_{22} &= \frac{(2\pi d)^{-2}\rho B N_0}{\sin^2(\zeta)\,\boldsymbol{c}_\rho^H\left(\boldsymbol{R}_1'' - \cos(2\pi d\cos(\zeta))\boldsymbol{R}_2''\right)\boldsymbol{c}_\rho}\\ [\boldsymbol{F}_q(\boldsymbol{\theta})^{-1}]_{33} &= \frac{1}{4}\frac{\rho B N_0}{\partial\boldsymbol{c}_\rho^H\left(\boldsymbol{R}_1'' + \cos(2\pi d\cos(\zeta))\boldsymbol{R}_2''\right)\partial\boldsymbol{c}_\rho}.\end{aligned} \tag{61}$$

For this general setup the performance measures are given by

$$\begin{aligned}\chi_\zeta(\boldsymbol{\theta}) &= \frac{(2d)^2}{\rho}\frac{\boldsymbol{c}_\rho^H\left(\boldsymbol{R}_1'' - \cos(2\pi d\cos(\zeta))\boldsymbol{R}_2''\right)\boldsymbol{c}_\rho}{\boldsymbol{c}^H\boldsymbol{c}}\\ \chi_\tau(\boldsymbol{\theta}) &= \frac{1}{\rho}\frac{\partial\boldsymbol{c}_\rho^H\left(\boldsymbol{R}_1'' + \cos(2\pi d\cos(\zeta))\boldsymbol{R}_2''\right)\partial\boldsymbol{c}_\rho}{\partial\boldsymbol{c}^H\partial\boldsymbol{c}}.\end{aligned} \tag{62}$$

In Fig. 6 the performance ratio of DOA estimation as function of the distance d and bandwidth ρ is highlighted. It can be seen that the gain which can be obtained by bandwidth reduction is becoming more significant (≈ 1 dB) when decreasing the antenna distance to $d = 0.2$. This means that the performance loss for the estimation of ζ due to compact antenna elements, can be partially recovered by reducing the bandwidth to $\rho = 0.58$. When considering time-delay estimation (Fig. 7) the importance of correctly choosing the analog filter bandwidth together with the antenna spacing can be seen clearly. In particular for a compact spacing of $d = 0.275$ and a reduced bandwidth of $\rho = 0.75$ we obtain a quantization-loss of only -0.5 dB at $\zeta = \pi/8$. Compared with the gains obtained separately in Fig. 4 for variable spacing and in Fig. 5 for variable bandwidth, the gain from the joint adjustment of both system parameters is more than additive.

VIII. Performance Analysis - Multiple Antennas

Finally, in order to investigate the performance behavior when using larger antenna arrays, we consider a ULA receiver with an odd number of antennas and steering vector

$$\boldsymbol{a}(\zeta) = \begin{bmatrix} e^{\mathrm{j}2\pi\mathrm{d}\frac{\mathrm{M}-1}{2}\cos(\zeta)} & \dots & 1 & \dots & e^{-\mathrm{j}2\pi\mathrm{d}\frac{\mathrm{M}-1}{2}\cos(\zeta)}\end{bmatrix}^T, \tag{63}$$

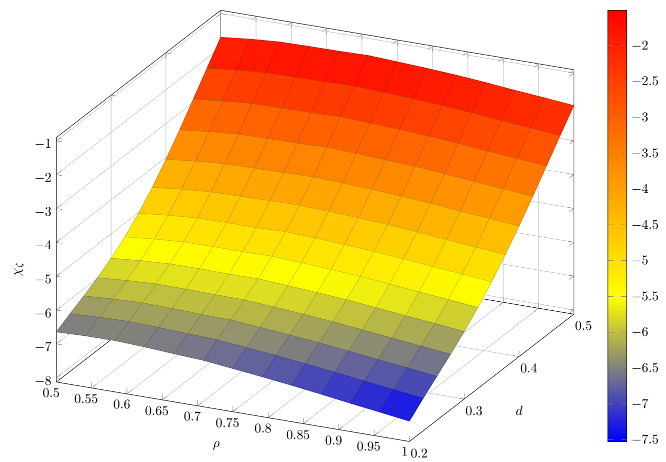

Fig. 6. 1-bit Performance Ratio in ζ (at $\zeta = \pi/8$) vs. Spacing and Bandwidth

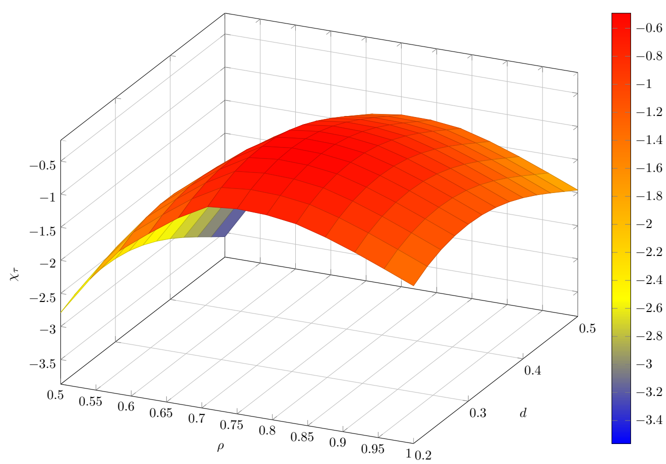

Fig. 7. 1-bit Performance Ratio in τ (at $\zeta = \pi/8$) vs. Spacing and Bandwidth

giving

$$\frac{\partial\boldsymbol{a}(\zeta)}{\partial\zeta} = \Big[-\mathrm{j}2\pi\mathrm{d}\frac{\mathrm{M}-1}{2}\sin(\zeta)\mathrm{e}^{\mathrm{j}2\pi\mathrm{d}\frac{\mathrm{M}-1}{2}\cos(\zeta)} \quad \dots \quad 0 \quad \dots \quad \mathrm{j}2\pi\mathrm{d}\frac{\mathrm{M}-1}{2}\sin(\zeta)\mathrm{e}^{-\mathrm{j}2\pi\mathrm{d}\frac{\mathrm{M}-1}{2}\cos(\zeta)}\Big]^{\mathrm{T}}. \tag{64}$$

Assuming all parameters except ζ to be known, it is possible to construct a simple lower bound on the estimation error of any unbiased DOA estimator [13]

$$\operatorname{var}(\hat{\zeta}) \geq \frac{1}{F_{q,\zeta}(\boldsymbol{\theta})}, \tag{65}$$

where

$$F_{q,\zeta}(\boldsymbol{\theta}) = 2\cdot\operatorname{Re}\left\{\frac{\partial\boldsymbol{s}^H(\boldsymbol{\theta})}{\partial\zeta}\boldsymbol{R}'\frac{\partial\boldsymbol{s}(\boldsymbol{\theta})}{\partial\zeta}\right\}, \tag{66}$$

is the Fisher information measure for the quantized receiver regarding ζ as function of the parameter constellation $\boldsymbol{\theta}$. Assuming the noise to be temporally white, i.e., $\boldsymbol{R}_T = BN_0\boldsymbol{I}$, the comparison to an unquantized system with $d = \frac{1}{2}$ takes the simple form

$$\chi_{q,\zeta}(\boldsymbol{\theta}) = \frac{F_{q,\zeta}(\boldsymbol{\theta})}{F_{\infty,\zeta}(\boldsymbol{\theta})\big|_{d=\frac{1}{2}}} = \frac{\frac{\partial \boldsymbol{a}^H(\zeta)}{\partial \zeta} \arcsin\left(\boldsymbol{C}_M\right)^{-1} \frac{\partial \boldsymbol{a}(\zeta)}{\partial \zeta}}{\left(\frac{\partial \boldsymbol{a}^H(\zeta)}{\partial \zeta}\frac{\partial \boldsymbol{a}(\zeta)}{\partial \zeta}\right)\Big|_{d=\frac{1}{2}}}. \tag{67}$$

This Fisher information ratio is given in Fig. 8 for different numbers of antennas. Contrary to the two antenna case, It can be observed that a significant performance improvement in DOA estimation can be achieved by slightly decreasing the antenna distance. In order to verify the effect of antenna spacing in the unquantized case, we use

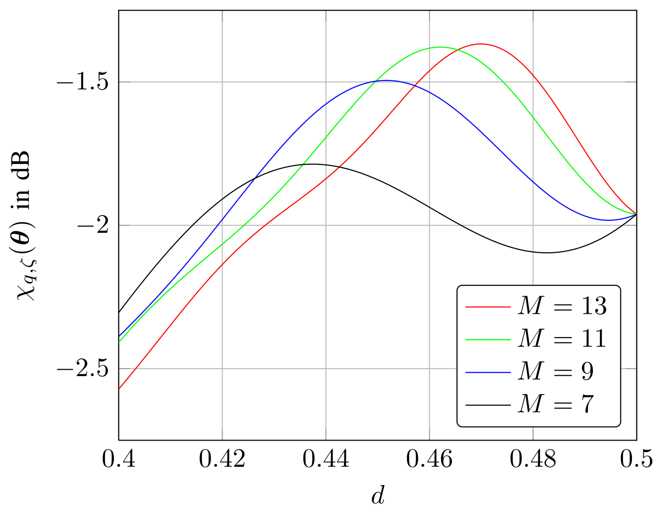

Fig. 8. 1-bit Performance Ratio in ζ (at $\zeta = \pi/8$) vs. Spacing

$$\chi_{\infty,\zeta}(\boldsymbol{\theta}) = \frac{F_{q,\zeta}(\boldsymbol{\theta})}{F_{\infty,\zeta}(\boldsymbol{\theta})\big|_{d=\frac{1}{2}}} = \frac{\frac{\partial \boldsymbol{a}^H(\zeta)}{\partial \zeta} \boldsymbol{C}_M^{-1} \frac{\partial \boldsymbol{a}(\zeta)}{\partial \zeta}}{\left(\frac{\partial \boldsymbol{a}^H(\zeta)}{\partial \zeta}\frac{\partial \boldsymbol{a}(\zeta)}{\partial \zeta}\right)\Big|_{d=\frac{1}{2}}}. \tag{68}$$

This performance benchmark is depicted in Fig. 9 for $M = 13$. Surprisingly, a huge performance improvement is obtained when decreasing the antenna spacing from $d = \frac{1}{2}$ to $d = \frac{1}{4}$ for DOAs close to the end-fire direction ($\zeta \approx 0$). This contradicts the general belief that decreasing the antenna distance degrades the DOA estimation performance.

IX. Conclusion

We have shown by means of a generic signal model, that the well-known -1.96 dB loss due to 1-bit quantization in the context of low-SNR array signal processing is not valid when noise correlation is present. In this work, we have analyzed this phenomenon under a general and physically consistent system model [9] [10]. Additionally, we have investigated the potential of jointly optimizing the analog receiver front-end, in particular the analog filter [7] and the antenna design [9] in order to create favorable noise correlation in a controlled way prior to the quantization device. An interesting observation of our analysis is the possible performance improvement for estimating several parameters by decreasing the antenna spacing below $\lambda/2$ for the ideal as well as for the 1-bit receiver case.

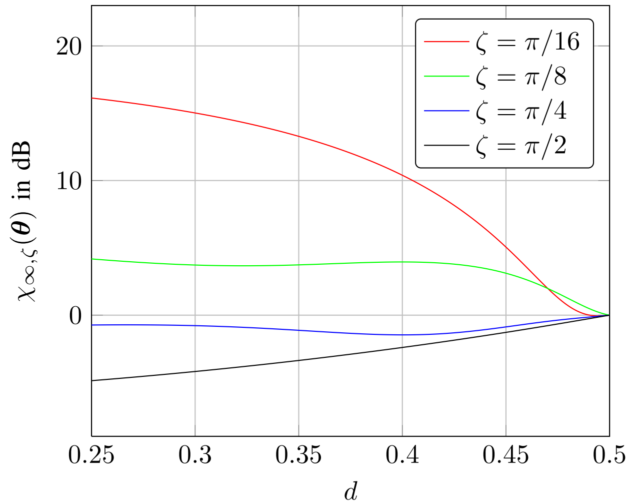

Fig. 9. Unquantized Performance Ratio in ζ ($M = 13$) vs. Spacing

Acknowledgment

The authors would like to thank Michel T. Ivrlač for discussions on physically consistent receiver models. The support of the German Federal Ministry of Economics and Technology through grant 50NA1110 is acknowledged.

References

[1] R. E. Curry, "Estimation And Control With Quantized Measurements," *M.I.T. Press*, 1970.

[2] J. H. Van Vleck, D. Middleton, "The spectrum of clipped noise," *Proceedings of the IEEE*, vol. 54, no. 1, pp. 2–19, 1966.

[3] J. W. Betz , N. R. Shnidman "Receiver processing losses with bandlimiting and one-bit sampling," in *Proceedings of the 20th International Technical Meeting of the Satellite Division of The Institute of Navigation (ION GNSS 2007)*, Texas, pp. 1244–1256, September 2007.

[4] A. Mezghani, J. A. Nossek, "Analysis of 1-bit Output Noncoherent Fading Channels in the Low SNR Regime," *IEEE International Symposium on Information Theory (ISIT)*, 2009.

[5] T. Koch, A. Lapidoth, "Increased capacity per unit-cost by oversampling," *IEEE 26th Convention of Electrical and Electronics Engineers in Israel (IEEEI)*, 2010

[6] J. T. Curran, D. Borio, G. Lachapelle, C. C. Murphy, "Reducing Front-End Bandwidth May Improve Digital GNSS Receiver Performance," *IEEE Transactions on Signal Processing*, vol. 58, no. 4, pp. 2399–2404, 2010.

[7] F. Wendler, M. Stein, A. Mezghani, J.A. Nossek, "Quantization-loss reduction for 1-bit BOC positioning," in *Proceedings of the ION International Technical Meeting*, January 2013.

[8] A. Mezghani, J. A. Nossek, "Capacity lower bound of MIMO channels with output quantization and correlated noise," *IEEE International Symposium on Information Theory Proceedings (ISIT)*, 2012.

[9] M. T. Ivrlač, J. A. Nossek, "Toward a Circuit Theory of Communication," *IEEE Transactions on Circuits and Systems I: Regular Papers*, vol. 57, no. 7, pp. 1663–1683, 2010.

[10] M. T. Ivrlač, J. A. Nossek, "On the Physical Meaning of the Model of Two Uncoupled Isotrops," in *Proceedings of the International ITG Workshop on Smart Antennas (WSA)*, 2012.

[11] A. Papoulis, "Probability, Random Variables, and Stochastic Processes," Third edition, *McGraw-Hill*, 1991.

[12] M. Stein, A. Mezghani, "On information measures and worst-case additive colored noise," *Technical Report, NWS-TUM*, 2012.

[13] S. M. Kay, "Fundamentals of Statistical Signal Processing: Estimation Theory," *Pretice Hall*, 1993.